Cellular Signalling 57 (2019) 89–101

Contents lists available at ScienceDirect

Cellular Signalling

journal homepage: www.elsevier.com/locate/cellsig

ER stress activation impairs the expression of circadian clock and clock-controlled genes in NIH3T3 cells via an ATF4-dependent mechanism

Lei Gao (高磊)[a,b,1], Huatao Chen (陈华涛)[a,b,*,1], Cuimei Li (李翠梅)[a,b], Yaoyao Xiao (肖要要)[a,b], Dan Yang (杨丹)[a,b,2], Manhui Zhang (张漫慧)[a,b], Dong Zhou (周栋)[a,b], Wei Liu (刘伟)[a,b], Aihua Wang (王爱华)[b,c], Yaping Jin (靳亚平)[a,b,*]

[a] Department of Clinical Veterinary Medicine, College of Veterinary Medicine, Northwest A&F University, Yangling 712100, Shaanxi, China
[b] Key Laboratory of Animal Biotechnology of the Ministry of Agriculture, Northwest A&F University, Yangling 712100, Shaanxi, China
[c] Department of Preventive Veterinary Medicine, College of Veterinary Medicine, Northwest A&F University, Yangling 712100, Shaanxi, China

ARTICLE INFO

Keywords:
Unfolded protein response
Circadian clock
Thapsigargin
Tunicamycin
4-Phenylbutyric acid

ABSTRACT

Endoplasmic reticulum (ER) stress and circadian clockwork signaling pathways mutually regulate various cellular functions, but the details regarding the cross-talk between these pathways in mammalian cells are unclear. In this study, whether perturbation of ER stress signaling affects the cellular circadian clockwork and transcription of clock-controlled genes was investigated in NIH3T3 mouse fibroblasts. An NIH3T3 cell model stably expressing luciferase (Luc) under the control of the *Bmal1* clock gene promoter was established using a lentiviral system. Then, Luc activity was monitored in real-time to detect *Bmal1-Luc* oscillations. The ER stress activators thapsigargin (Tg) and tunicamycin (Tm) markedly reduced *Bmal1-Luc* oscillation amplitudes and induced phase delay shifts in NIH3T3 cells. Treatment with Tg/Tm activated ER stress signaling by upregulating GRP78, CHOP, ATF6, and ATF4 and simultaneously significantly decreased BMAL1 protein levels and inhibited the transcription of circadian clock (*Bmal1*, *Per2*, *Nr1d1*, and *Dbp*) and clock-controlled (*Scad1*, *Fgf7*, and *Arnt*) genes. 4-Phenylbutyric acid, an ER stress inhibitor, alleviated the transcriptional repression of the circadian clock genes and partially restored *Bmal1-Luc* oscillation amplitudes in Tg- or Tm-treated NIH3T3 cells. More importantly, knock-down of ATF4, but not ATF6, in Tg-treated NIH3T3 cells partially rescued *Bmal1-Luc* oscillation amplitudes and mRNA expression of the four circadian clock genes. Taken together, our study demonstrates that ER stress activation inhibits the transcription of circadian clock and clock-controlled genes via an ATF4-dependent mechanism.

1. Introduction

The endoplasmic reticulum (ER) is a large membrane-bound organelle involved in protein biosynthesis, providing a suitable oxidative environment for the folding and maturation of membrane and secretory proteins in mammalian cells [1,2]. However, when protein processing and folding requirements exceed the capacity of the ER, unfolded proteins accumulate, evoking ER stress and inducing the unfolded protein response (UPR) [3]. The UPR is a concerted and complex cellular response mediated through three ER stress transducers: inositol-requiring enzyme 1 (IRE1), protein kinase RNA-like ER kinase (PERK), and activating transcription factor 6 (ATF6) [4]. Under non-stress conditions, the three transducers are maintained in a relatively inactive state through association with the glucose-regulated protein 78 (GRP78) ER chaperone. Under stress conditions, however, physiological and/or pathological stress signals (protein degradation, calcium

Abbreviations: ER, Endoplasmic reticulum; UPR, unfolded protein response; IRE1, inositol-requiring enzyme 1; PERK, protein kinase RNA-like ER kinase; ATF6, activating transcription factor 6; GRP78, glucose-regulated protein 78; eIF2α, eukaryotic translation initiation factor 2α; CHOP, C/EBP homologous protein; XBP1, X-box binding protein 1; S1P, site-1 protease; S2P, site-2 protease; Tg, thapsigargin; Tm, tunicamycin; 4-PBA, 4-Phenylbutyric acid; SCN, suprachiasmatic nucleus; siRNA, small interfering RNA; DXM, dexamethasone

* Corresponding authors at: Department of Clinical Veterinary Medicine, College of Veterinary Medicine, Northwest A&F University, Yangling 712100, Shaanxi, China.
E-mail addresses: htchen@nwafu.edu.cn (H. Chen), yapingjin@163.com (Y. Jin).
[1] Lei Gao and Huatao Chen are regarded as co-first authors.
[2] Present Address: Laboratory of Regulation in Metabolism and Behavior, Graduate School of Agriculture, Kyushu University, Fukuoka, Japan.

https://doi.org/10.1016/j.cellsig.2019.01.008
Received 8 November 2018; Received in revised form 25 January 2019; Accepted 25 January 2019
Available online 28 January 2019
0898-6568/

imbalance, hypoxia, and cellular redox dysregulation) alter calcium homeostasis and elicit an accumulation of misfolded proteins in the ER [5]. This accumulation leads to GRP78 dissociation and activation of the three transducers, triggering the pro-survival UPR to reduce the backlog of unfolded proteins and restore normal ER function [6].

Upon release from GRP78, PERK is autophosphorylated, resulting in a cascade of signals including phosphorylation of eukaryotic translation initiation factor 2α (eIF2α) and translation of ATF4, which elicits transcription of C/EBP homologous protein (CHOP) [7–9]. Under ER stress, IRE1 is activated by autophosphorylation, which facilitates the splicing of a 26-base intron from X-box binding protein 1 (XBP1) mRNA [10]. Spliced (s) XBP1 upregulates ER chaperone genes as well as other components to assist in the folding capacity of the ER [11]. ATF6 translocates from the ER to the Golgi apparatus, where it is cleaved by the site-1 and site-2 proteases (S1P and S2P) [12]. The cleaved ATF6 N-terminal fragment is then transported to the nucleus and acts in combination with ATF4 and sXBP1 to increase the levels of proteins and alleviate ER stress.

To investigate the interface between ER stress signaling and other signaling pathways, various agents are commonly used to modulate ER stress signals in cells. Thapsigargin (Tg) is a non-competitive inhibitor of the ER Ca^{2+} ATPase that when applied restricts Ca^{2+} transport to the ER, resulting in ER stress due to the depletion of Ca^{2+} from the ER lumen [13,14]. Similarly, tunicamycin (Tm), a mixture of homologous nucleoside antibiotics, induces the UPR by blocking N-linked glycosylation in the ER [13,15,16]. In addition, the chemical chaperone 4-Phenylbutyric acid (4-PBA) is an ER stress inhibitor that attenuates ER stress both in vivo and in vitro [17,18]. We previously described that the Tg and Tm ER stress activators, as well as the 4-PBA inhibitor, effectively modify ER stress in goat cells in vitro [19].

In mammals, the circadian clock system encompasses nearly all organs, tissues, and cells [20]. Various diurnal changes in physiological functions and behaviors, including the sleep/wake cycle, feeding, body temperature, blood pressure, and release of endocrine hormones, are driven by an endogenous circadian clockwork [21]. The central pacemaker that controls circadian rhythms is located in the suprachiasmatic nucleus (SCN) of the hypothalamus [22]. The SCN is synchronized primarily with environmental time in the 24-h light-dark cycle and orchestrates subsidiary circadian oscillators in peripheral tissues and cells using humoral and neuronal cues in a hierarchical manner [23,24]. At the molecular level, the circadian clockwork underlying the generation of circadian rhythms is composed of a conservative interlocked transcriptional-translational feedback loop comprising a set of circadian clock genes [25]. The transcriptional activators BMAL1 and CLOCK dimerize and drive the transcription of the Period (*Per1*, *Per2*, and *Per3*) and Cryptochrome (*Cry1* and *Cry2*) genes. After translation, PER and CRY proteins oligomerize and translocate to the nucleus where they inhibit BMAL1/CLOCK activity as well as their own transcription. An auxiliary essential feedback loop that includes orphan nuclear receptors (REV-ERBs and ROR) and the DBP proteins makes circadian oscillators more robust and tunable [5].

The ER stress and circadian clockwork signaling pathways both play important roles in regulating various physiological processes including apoptosis, autophagy, steroid hormone secretion, and lipid metabolism [26–35]. These pathways share similar physiological roles in regulating cellular processes, suggestive of cross-talk between the two pathways. Indeed, recent reports have provided evidence of molecular connections between ER stress and circadian clockwork signaling. Regarding circadian clock-mediated regulation of ER stress, one study showed that the rhythmic activation of IRE1α by the circadian clock-coordinated 12-h period controls lipid metabolism in the mouse liver [36]. Moreover, a different study reported that the *Clock* circadian gene regulates ER stress and senescence by controlling the transcription of a clock-controlled gene, *Pdia3* [37]. In contrast, very recent evidence revealed that PERK, a major ER stress sensor, induces miR-211, which transiently inhibits the core circadian regulators *Bmal1* and *Clock*, highlighting that ER stress signaling regulates the circadian clock [38].

Relatively few studies have investigated the relationship between ER stress and the circadian clockwork, and the associated regulatory mechanisms remain unclear. In the present study, we assessed whether perturbation of ER stress signaling by ER stress activators (Tg and Tm) and an ER stress inhibitor (4-PBA) in NIH3T3 mouse fibroblast cells alters the expression of circadian clock and clock-controlled genes. We also used real-time monitoring of the circadian clock gene *Bmal1* promoter-driven bioluminescence and cell-based small interfering RNA (siRNA) knockdown to uncover the mechanisms by which ER stress regulates the cellular circadian clock. The results demonstrate that ER stress activation inhibits the transcription of cellular circadian clock and clock-controlled genes via the ATF4 signaling axis. The findings extend the knowledge of the cross-talk between the circadian clock and ER stress signaling pathways.

2. Materials and methods

2.1. Cell culture

NIH3T3 mouse fibroblasts were obtained from The Cell Bank of Type Culture Collection of Chinese Academy of Sciences (Shanghai, China). The cells were cultured in high-glucose Dulbecco's modified Eagle's medium (DMEM; Gibco, Grand Island, NY, USA) supplemented with 10% fetal bovine serum (FBS; Gibco), 1× antibiotic-antimycotic (AA, containing penicillin, streptomycin, and amphotericin B; Invitrogen, Carlsbad, CA, USA) in a humidified atmosphere with 5% CO_2 at 37 °C. Cells were cultured for 24 h before treatment unless otherwise stated.

2.2. Determination of appropriate Tg and Tm treatment concentrations in NIH3T3 cells

NIH3T3 cells were plated in 96-well plates and cultured for 24 h until confluence. Thapsigargin (Sigma-Aldrich, St. Louis, MO, USA) was added to cells at a concentration of 0, 20, 60, 180, 540, or 1620 nM for 12 or 32 h. Similarly, Tm (Sigma-Aldrich) was added at 0, 20, 60, 180, 540, or 1620 ng/mL for the same periods of time. A Cell Counting Kit-8 (CCK-8; Beyotime, Shanghai, China) was used to assay cell viability. The maximum concentrations of Tg and Tm that did not significantly affect cell viability were selected as the treatment concentrations.

2.3. Immunofluorescence assay

The immunofluorescence assay was performed according to previously described methods [39]. Briefly, NIH3T3 cells were seeded on 15-mm diameter glass coverslips in 24-well plates. After 24 h, the cells were synchronized with 100 nM dexamethasone (DXM) for 2 h and then left untreated (control, Cont) or were treated with Tg or Tm at the indicated concentrations (the addition of Tg or Tm was designated 0 h). Control or Tg-/Tm-treated cells were washed twice with phosphate buffered saline (PBS) and fixed with 4% paraformaldehyde at 25 °C for 20 min at three representative time points (0, 12, and 32 h). After three washes with PBS, the cells were permeabilized with 0.1% Triton X-100 in PBS (PBST) for 30 min at 25 °C and subsequently blocked for 30 min with 5% bovine serum albumin in PBS at 25 °C. The cells were incubated overnight at 4 °C with rabbit anti-GRP78 antibody (Proteintech, Rosemont, IL, USA) diluted 1:200. Rabbit serum (Abcam, Cambridge, MA, USA) was substituted for the primary antibody for the negative control. The cells were then washed in PBS, incubated for 1 h at 37 °C in donkey anti-rabbit IgG (H + L) highly cross-adsorbed secondary antibody (Alexa Fluor 488; Thermo Fisher Scientific, Waltham, MA, USA) diluted 1:200 in PBS, and washed again with PBST. Nuclei were stained with 2 μg/mL 4′,6-diamidino-2-phenylindole dihydrochloride (DAPI; Thermo Fisher Scientific) for 5 min. The fluorescent signals were detected using an A1Rsi confocal microscope system

(Nikon Corporation, Tokyo, Japan).

2.4. Real-time monitoring of Bmal1-Luc oscillations

NIH3T3 cells stably expressing luciferase (Luc) under the control of the *Bmal1* promoter were first established using a lentiviral system following previously published procedures [40]. The recombinant lentiviral vector *pLV6-Bmal1-Luc* was a gift from Steven Brown (Addgene plasmid # 68833). Briefly, the *pLV6-Bmal1-Luc* and lentivirus package vectors encoding Gag-Pol, Rev., and Vsv-G were co-transfected into 293 T cells using the TurboFect Transfection Reagent (Thermo Fisher Scientific). The supernatant was collected and filtered through a 0.45-μm polyvinylidene fluoride (PVDF) filter after transfection. Viruses were concentrated 10-fold by ultracentrifugation. NIH3T3 cells were infected with lentivirus that was diluted into the medium with 8 μg/mL polybrene. After 16 h, the culture medium containing the lentivirus was changed to fresh complete culture medium. Blasticidin was used to select for positive clones that were stably transfected by *pLV6-Bmal1-Luc*. Cells that stably expressed luciferase under the control of the *Bmal1* promoter were maintained in high-glucose DMEM supplemented with 10% FBS and 1× AA at 37 °C in 5% CO_2 for 24 h until confluence. For Tg/Tm treatment, cells were then administered 100 nM DXM for 2 h and the medium was then changed to phenol red-free DMEM supplemented with 10% FBS, 0.1 mM luciferin (Thermo Fisher Scientific), and 1× AA in the presence or absence of Tg (60 nM) or Tm (60 ng/mL). For 4-PBA treatment, cells were treated with 100 nM DXM for 2 h and the medium was changed to phenol red-free DMEM supplemented with 10% FBS, 0.1 mM luciferin, and 1× AA in the presence or absence of Tg (60 nM)/Tm (60 ng/mL) with or without co-administration of 4-PBA (1 μM). For ATF6 knockdown, cells were maintained in transfection medium with *Atf6* siRNAs or non-silencing control RNAs (NC) for 12 h, and then treated with 100 nM DXM for 2 h. The *Atf6* siRNA-treated cells were further administered 60 nM Tg, and the NC cells were administered 60 nM Tg or not. For ATF4 knockdown, cells were maintained in transfection medium with *Atf4* siRNAs or NC RNAs for 12 h, and then treated with 100 nM DXM for 2 h. The *Atf4* siRNA-treated cells were further administered 60 nM Tg, and the NC cells were administered 60 nM Tg or not. Luciferase activity was monitored over time at 37 °C with a Kronos Dio AB-2550 luminometer (ATTO, Tokyo, Japan) interfaced to a computer for continuous data acquisition, as previously described [41]. The data are presented as photon counts per min, calculated at 9 min intervals. A baseline correction was calculated using a 24-h moving average, which removed the first 12 h of data. The time of the second phase was determined from the peak that appeared between 24 h and 48 h of culture after DXM synchronization. The *Bmal1-Luc* amplitude was documented by the single cosinor method using Time Series Analysis Serial Cosinor 6.3 Software (Expert Soft Tech, Richelieu, France).

2.5. Protein extraction and western blotting

Preparation of whole-cell lysates from NIH3T3 cells and western blotting procedures were performed as previously described [42]. For the ER stress activation experiment, NIH3T3 cells synchronized or not with 100 nM DXM for 2 h were treated with Tg or Tm at the indicated concentrations. Cells were harvested at three representative time points (0, 12, and 32 h after Tg or Tm treatment). For the 4-PBA-mediated ER stress-alleviating experiment, non-synchronized NIH3T3 cells were treated with Tg, Tm, Tg + 4-PBA, or Tm + 4-PBA. Cells were harvested 24 h after treatment. Cell sediments were washed with cold PBS and lysed using a radioimmunoprecipitation assay buffer containing protease inhibitors. The protein concentrations of the cell lysates were determined using a bicinchoninic acid assay. Total cellular proteins were extracted with a 5× sodium dodecyl sulfate polyacrylamide gel electrophoresis (SDS-PAGE) loading buffer after boiling in water for 5 min. Equal volumes of total cellular protein were resolved using 12% SDS-PAGE and electrotransferred onto PVDF membranes. After blocking with 10% non-fat milk for 1 h in Tris-buffered saline containing 0.5% Tween 20 (TBST) at 25 °C, the membranes were incubated with primary antibodies diluted in TBST overnight at 4 °C, and then with horseradish peroxidase (HRP)-conjugated secondary antibodies diluted in TBST at 25 °C for 1 h. Finally, the membranes were washed five times in TBST for 5 min. Peroxidase activity was detected using a WesternBright ECL HRP substrate kit (Advansta, Menlo Park, CA, USA). The immunoreactive bands were visualized using a Gel Image System (Tannon Biotech, Shanghai, China) and digitized with Quantity One software (Bio-Rad Laboratories, Hercules, CA, USA). The primary antibodies used were: rabbit anti-GRP78 (Cell Signaling Technology, Danvers, MA, USA; 1:1000), mouse anti-CHOP (Abcam, Cambridge, MA, USA; 1:1000), rabbit anti-ATF4 (Proteintech, Rosemont, IL, USA; 1:1000), rabbit anti-ATF6 (Abcam; 1:1000), rabbit anti-phospho-IRE1 (Abcam; 1:1000), rabbit anti-BMAL1 (Abcam; 1:2000), and mouse anti-β-actin (Sanjian Biotech, Tianjin, China; 1:2000). The secondary antibodies used were: HRP-conjugated goat anti-rabbit (Zhongshan Golden Bridge Biotechnology, Nanjing, China; 1:5000) and HRP-conjugated goat anti-mouse (Zhongshan Golden Bridge Biotechnology; 1:5000).

2.6. siRNA transfection

Each of the three sequences targeting mouse *Atf6* mRNA, *Atf4* mRNA, and their scrambled RNAs (non-silencing RNAs as negative controls, NC) were purchased from GenePharma (Shanghai, China). The RNA oligo sequences used for *Atf6* and *Atf4* are listed in Table 1 and Table 2, respectively. NIH3T3 cells were first plated in 35-mm dishes with 2 mL DMEM supplemented with 10% FBS and 1× AA. After 24 h in culture, the medium was removed and the *Atf6* and *Atf4* siRNAs, as well as the non-silencing RNAs, diluted in Opti-MEM, were transfected into cells using TurboFect transfection reagent according to the manufacturer's protocol. The *Atf6* and *Atf4* siRNAs, and the non-silencing RNA, were used at a final concentration of 25 nM. The cells were maintained in transfection medium for 12 h. To verify siRNA knockdown efficiency, the medium was replaced with medium supplemented with 10% FBS and 1× AA. After 48 h, the cells were harvested for total RNA and protein extraction. For the siRNA + Tg treatment, the medium was replaced with medium supplemented with 10% FBS and 1× AA in the presence or absence of Tg. Cells were divided into three groups: negative control (NC), NC + Tg treatment (Tg), and Tg + *Atf6* or *Atf4* siRNA (Tg + Si). After 48 h, the cells were harvested for total RNA and protein extraction.

2.7. RNA extraction and real-time quantitative PCR

The differently treated cells were harvested at the indicated time points. Total RNA was extracted using TRIzol reagent (TaKaRa, Dalian, China). RNA samples were treated with RNase-free DNase (TianGen, Beijing, China). The cDNAs were generated using the PrimeScript RT Reagent Kit (TaKaRa). The primer sets used for the real-time quantitative PCR (qPCR) are listed in Table 3. All primer sets were designed to span introns to avoid amplifying products from genomic DNA. The

Table 1
siRNA sequences targeting *Atf6* mRNA.

	siRNA Sequence 5′-3′
siRNA1	F:GCACUUUGAUGCAGCACAUTT R:AUGUGCUGCAUCAAAGUGCTT
siRNA2	F:GCAGUCGAUUAUCAGCAUATT R:UAUGCUGAUAAUCGACUGCTT
siRNA3	F:GCCACCAGAAGUAUGGGUUTT R:AACCCAUACUUCUGGUGGCTT
Negative control	F:UUCUCCGAACGUGUCACGUTT R:ACGUGACACGUUCGGAGAATT

Table 2
siRNA sequences targeting *Atf4* mRNA.

	siRNA Sequence 5′-3′
siRNA1	F:CCUGGAAACCAUGCCAGAUTT R:AUCUGGCAUGGUUUCCAGGTT
siRNA2	F:CCACUCCAGAGCAUUCCUUTT R: AAGGAAUGCUCUGGAGUGGTT
siRNA3	F:GCCCAAACCUUAUGACCCATT R:UGGGUCAUAAGGUUUGGGCTT
Negative control	F:UUCUCCGAACGUGUCACGUTT R:ACGUGACACGUUCGGAGAATT

qPCR was performed in a 20 μL reaction volume containing 10 ng cDNA and SYBR® Premix Ex Taq II (TaKaRa) and 200 nM specific primers using the CFX96 RT-qPCR system (Bio-Rad), according to the parameters described in our previous report [43]. Melting peaks were determined with melting curve analysis to ensure amplification of a single product. All reactions were performed in triplicate and displayed amplification efficiencies of between 80% and 120%. The $2^{-\triangle\triangle Ct}$ method was used to quantify gene expression. The relative quantity for each sample was normalized to the average level of the constitutively expressed housekeeping gene *36b4*.

2.8. Data and statistical analyses

Data are expressed as the means ± SE of at least three separate experiments, each performed in triplicate. Statistical analyses were performed by two-way ANOVA or Student's *t*-test, as indicated, using SigmaPlot 12.0 (Systat Software, San Jose, CA, USA). Differences were considered significant at $P < 0.05$.

3. Results

3.1. Tg/Tm treatment evokes ER stress signaling in NIH3T3 cells

To investigate the potential role of ER stress signaling in regulating cellular circadian clockwork, ER stress activation models were first established in NIH3T3 cells using the two classical ER stress activators, Tg and Tm. The appropriate Tg and Tm treatment concentrations were screened using a CCK-8 assay. The assay results showed that the maximum Tg and Tm treatment concentrations that did not significantly affect cell viability at 12 h and 32 h compared to the Cont group were 60 nM and 60 ng/mL, respectively (Supplemental Fig. 1). A prior report showed that Tg at 100 nM and Tm at 100 ng/mL increased the expression of the ER chaperone GRP78, commonly used as an ER stress marker, in NIH3T3 cells [44]. Based on the present and previous results, Tg and Tm treatment concentrations were determined to be 60 nM and 60 ng/mL, respectively.

After treatment with 60 nM Tg or 60 ng/mL Tm, the expression and distribution of the GRP78 protein in NIH3T3 cells were examined using immunofluorescence at three representative time points (0, 12, and 32 h). As shown in Fig. 1, immunostaining results revealed that both Tg and Tm treatments strikingly increased GRP78 expression at 12 and 32 h with a uniform distribution in both the cytoplasm and nucleus of NIH3T3 cells, compared with the weak signal observed in the 0, 12, and 32 h Cont groups, indicating the establishment of ER stress activation models in NIH3T3 cells.

3.2. Effects of Tg/Tm treatment on Bmal1-Luc oscillations in NIH3T3 cells after DXM synchronization

The NIH3T3 cell model stably expressing *Luc* under the control of the *Bmal1* promoter was established using a lentivirus system. To examine whether Tg/Tm-evoked ER stress impaired the cellular circadian clockwork, *Bmal1-Luc* oscillations in NIH3T3 cells were monitored using a luminometer in the presence or absence of Tg or Tm after DXM synchronization. *Bmal1-Luc* oscillations were clearly observed both in the presence and absence of Tg or Tm (Fig. 2A). Interestingly, both Tg and Tm markedly dampened the amplitude of *Bmal1-Luc* oscillations compared to the Cont group (Fig. 2A and C). Tm, but not Tg, lengthened the period of *Bmal1-Luc* oscillations compared to the Cont group (Fig. 2C). Additionally, both Tm and Tg induced *Bmal1-Luc* oscillation phase delay shifts in the peak time of the second phase compared to the Cont group (Fig. 2A and B). These findings support that ER stress activation in NIH3T3 cells damages the cellular circadian clockwork.

3.3. Tg-/Tm-induced ER stress activation downregulates BMAL1 protein levels in NIH3T3 cells

To verify the successful establishment of ER stress activation cell models, the protein levels (GRP78, CHOP, ATF4, ATF6, and phospho-IRE1) in the canonical ER stress signaling pathways in NIH3T3 cells following Tg or Tm treatment were examined using western blotting.

Table 3
Primer sequences for the genes targeted in qPCR.

Target gene	GenBank accession no.	Primer sequence 5′-3′	Product size (bp)
mBmal1	NM_007489.4	F:AGGCGTCGGGACAAAATGAACA R:TGGGTTGGTGGCACCTCTCA	147
mNr1d1	NM_145434.4	F:TGGCATGGTGCTACTGTGTAAGG R:ATATTCTGTTGGATGCTCCGGCG	114
mPer2	NM_011066.3	F: CCATCCACAAGAAGATCCTAC R: GCTCCACGGGTTGATGAAGC	128
mDbp	NM_016974.3	F:AATGACCTTTGAACCTGATCCCGCT R:GCTCCAGTACTTCTCATCCTTCTGT	175
mClock	NM_001305222.1	F:CACTCTCACAGCCCCACTGTAC R:CCCCACAAGCTACAGGAGCAGT	200
mArnt	NM_009709.4	F:GCATGGGCTCACGAAGGT R:AACAGGGTCCACGGAGCTAGT	56
mFgf7	NM_008008.4	F:AAGGGACCCAGGAGATGAAGA R:TGCCACAATTCCAACTGCC	71
mScad1	NM_009127.4	F:AACACCATGGCGTTCCAAA R:GGTGGGCGCGGTGAT	58
mAtf6	NM_001081304.1	F:TCGCCTTTTAGTCCGGTTCTT R:GGCTCCATAGGTCTGACTCC	190
mAtf4	NM_001287180.1	F:ACCATGGCGTATTAGAGGCAG R:ACACTGCTGCTGGATTTCGT	134
m36b4	NM_007475.5	F:CTCACTGAGATTCGGGATATG R: CTCCCACCTTGTCTCCAGTC	223

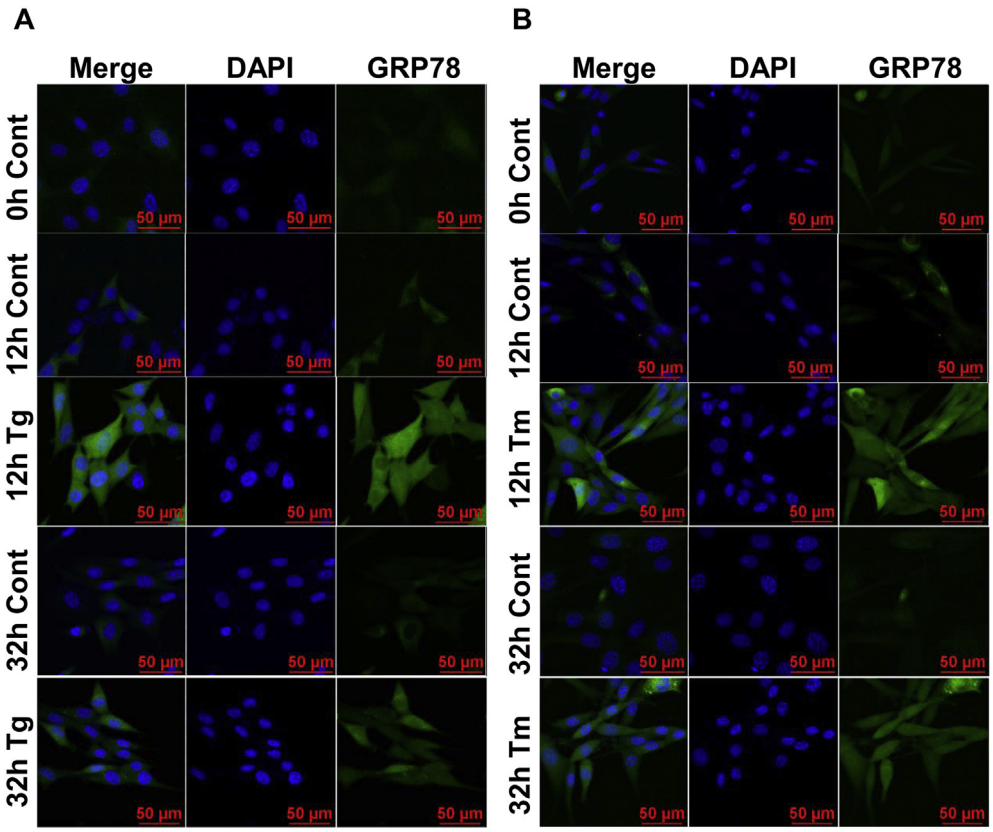

Fig. 1. Immunofluorescence analysis of GRP78 expression in NIH3T3 cells after Tg/Tm treatment.
Cells were subjected to immunofluorescence analysis using an anti-GRP78 antibody (green) and DAPI (blue) staining. The GRP78 staining intensity was increased at 12 h and 32 h after treatment with Tg (60 nM) or Tm (60 ng/mL) compared to the Cont group. Images are representative of three separate tests performed at each time point.

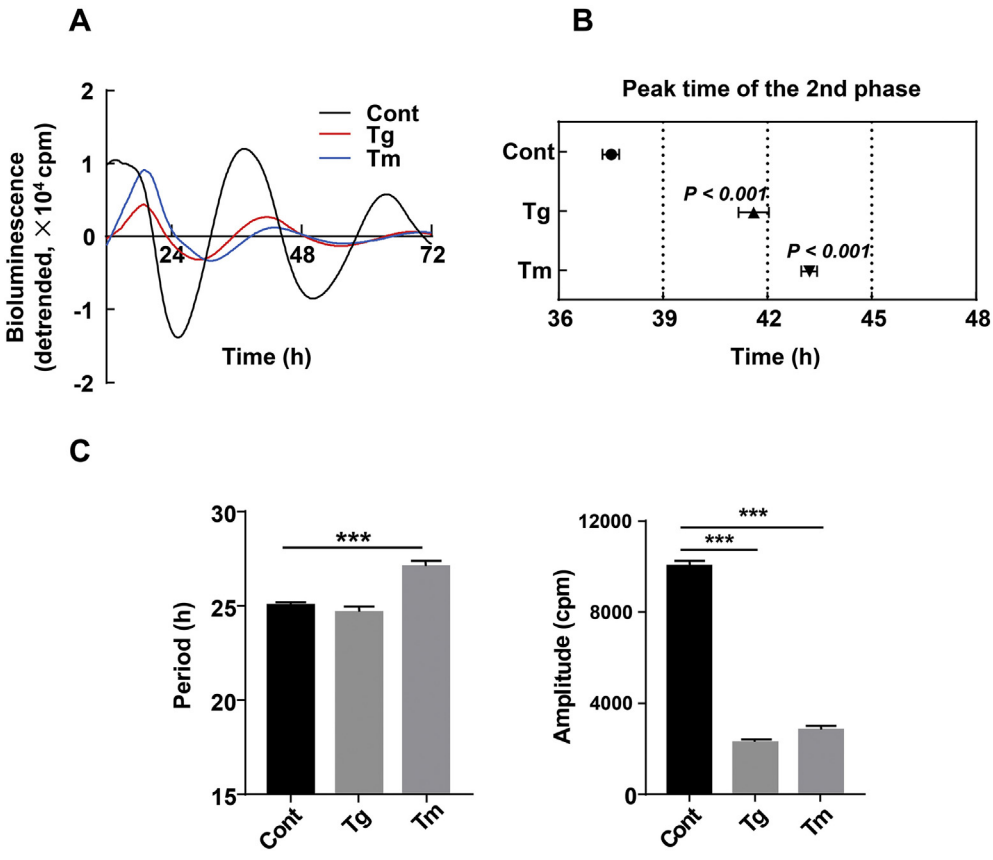

Fig. 2. Effect of Tg or Tm treatment on *Bmal1-Luc* oscillations in NIH3T3 cells.
A: Representative bioluminescence recordings showing the effect of Tg and Tm on *Bmal1-Luc* oscillations in NIH3T3 cells. The NIH3T3 cells were first synchronized using 100 nM DXM, then bioluminescence was determined in the presence or absence of Tg (60 nM) or Tm (60 ng/mL). B: Peak time of the second phase in NIH3T3 cells in the presence or absence of Tg or Tm. Each point represents the mean ± SE ($n = 6$). Differences were considered significant at $P \leq 0.05$. C: Period and amplitude of *Bmal1-Luc* oscillations in NIH3T3 cells with or without Tg or Tm treatment. Period and amplitude were generated by the cosinor method based on data for the first 72 h. Results are the means ± SE (n = 6). *** $P < 0.001$ vs. Cont.

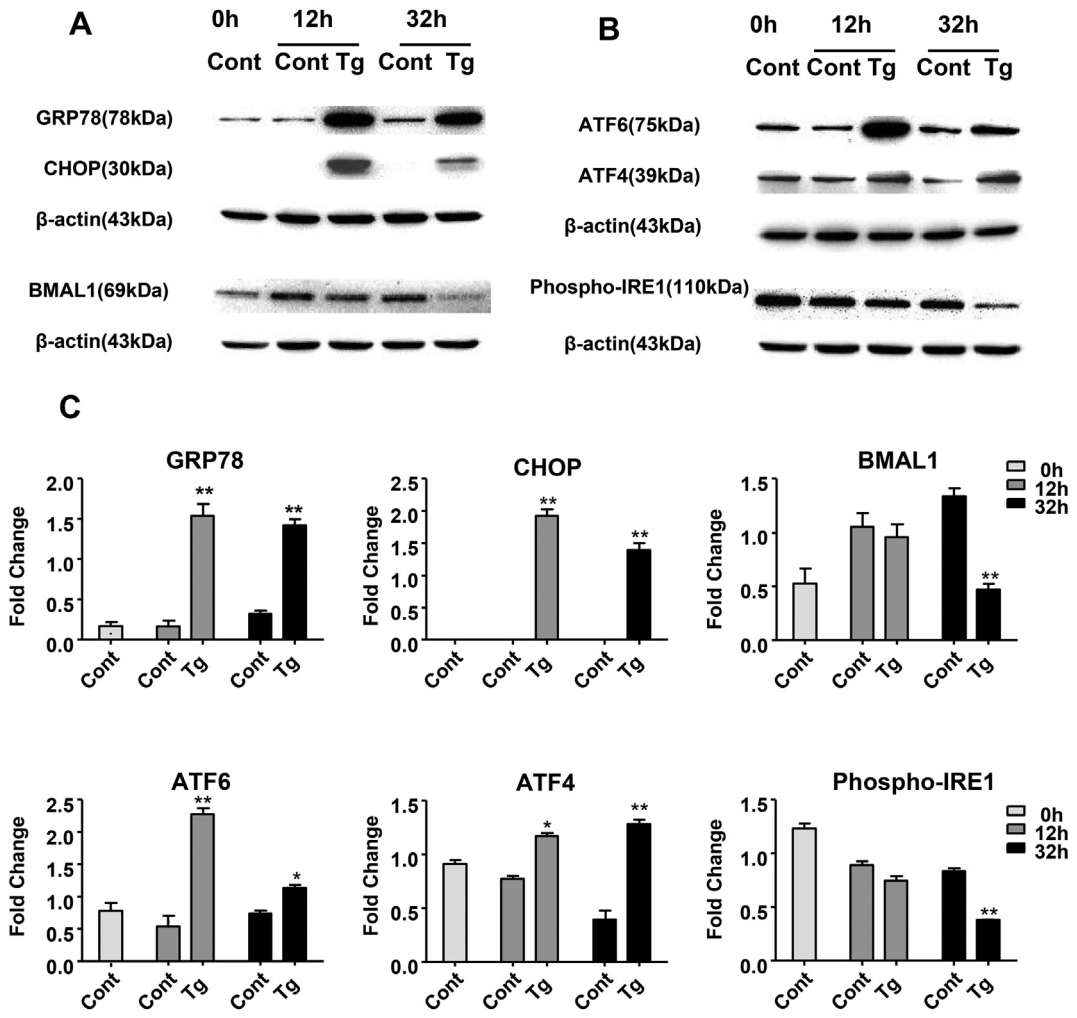

Fig. 3. Effect of Tg treatment on protein levels related to the ER stress and circadian clock signaling pathways in NIH3T3 cells.
NIH3T3 cells were first synchronized using 100 nM DXM for 2 h, and were then treated with 60 nM Tg. Cell sediments were collected at the indicated times and subjected to western blotting analysis. A and B: Expression of GRP78, CHOP, BMAL1, ATF6, ATF4, and phospho-IRE1 in NIH3T3 cells treated or not with Tg at the indicated times. C: The ratio of each protein to β-actin was determined from the densities of the immunoreactive bands, and the results are shown as a bar graph. All data are presented as the means ± SE ($n = 3$). * $P < 0.05$, ** $P < 0.01$ vs. Cont at each time point.

Thapsigargin administration significantly increased GRP78, CHOP, ATF4, and ATF6 protein levels in synchronized NIH3T3 cells at 12 and 32 h after treatment, but decreased the level of phospho-IRE1 at 32 h (Fig. 3A–C). Interestingly, Tg treatment led to the downregulation of BMAL1 expression in synchronized NIH3T3 cells at 32 h and in non-synchronized NIH3T3 cells at both 12 and 32 h after treatment (Fig. 3A, C; Supplemental Fig. 2A, B). Similarly, Tm also significantly elevated GRP78, CHOP, ATF4, and ATF6 protein levels in synchronized NIH3T3 cells (Fig. 4A–C). Notably, Tm administration significantly decreased the phospho-IRE1 level at 12 h and increased the phospho-IRE1 level at 32 h after treatment (Fig. 4 B, C). In addition, a decrease in the BMAL1 protein levels was clearly observed in both synchronized and non-synchronized NIH3T3 cells after Tm treatment (Fig. 4A, C; Supplemental Fig. 2C, D). These results demonstrated the successful establishment of ER stress activation in NIH3T3 cells, providing further evidence that ER stress activation by Tg/Tm treatment impairs the cellular circadian clockwork.

3.4. Tg-/Tm-mediated ER stress activation impairs circadian clock and clock-controlled gene transcription in NIH3T3 cells

To further examine whether ER stress evoked by Tg/Tm can impair the circadian clockwork in NIH3T3 cells, the mRNA expression profiles of circadian clock and clock-controlled genes in DXM-synchronized NIH3T3 cells with or without Tg/Tm treatment were measured using RNA samples collected at the indicated time points (sampling time corresponded to the first *Bmal1-Luc* oscillation between 12 and 32 h). The results are presented in Fig. 5. Treatment with both Tg and Tm strikingly reduced the mRNA levels of circadian clock genes (*Bmal1*, *Per2*, and *Nr1d1*) and clock-controlled genes (*Scad1*, *Fgf7*, and *Arnt*) (two-way ANOVA, $P < 0.001$). *Clock* expression was weakly reduced following Tg treatment (Fig. 5A, two-way ANOVA, $P < 0.001$). Thapsigargin inhibited *Dbp* mRNA expression (Fig. 5A, two-way ANOVA, $P < 0.001$), while Tm delayed the phase of *Dbp* mRNA expression (Fig. 5B). The data showed that Tg-/Tm-induced ER stress activation impaired the transcription of cellular circadian clock and clock-controlled genes, indicating a potential role for ER stress in regulating the cellular circadian clockwork.

3.5. 4-PBA attenuates the inhibitory effect of Tg-/Tm-mediated ER stress activation on the transcription of circadian clock genes and Bmal1-Luc oscillation amplitude

The chemicals Tg and Tm are ER stress activators that induce ER stress through different specific mechanisms. Thapsigargin evokes ER stress by inhibiting Ca^{2+} transport to the ER lumen, while Tm elicits ER

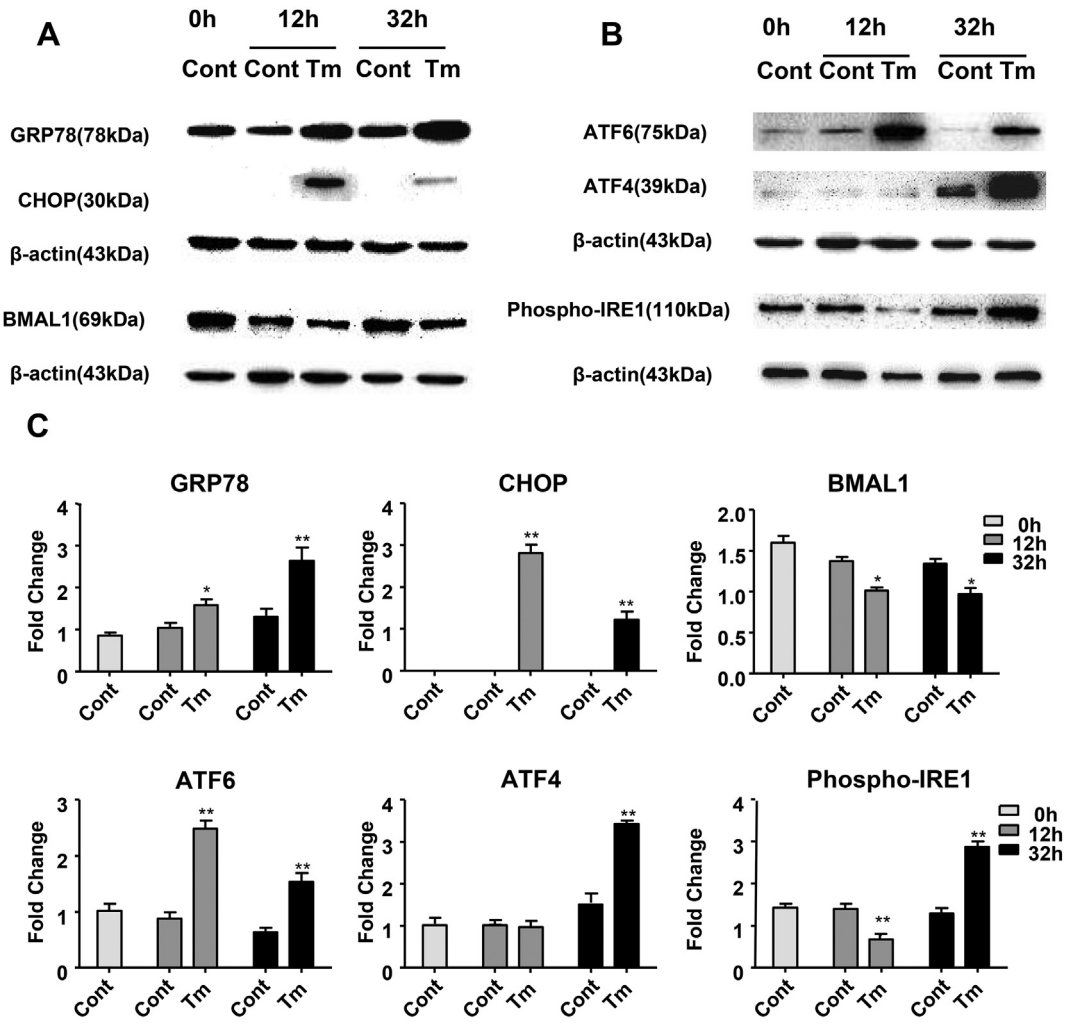

Fig. 4. Effect of Tm treatment on protein levels related to the ER stress and circadian clock signaling pathways in NIH3T3 cells.
NIH3T3 cells were first synchronized using 100 nM DXM for 2 h, and were then treated with 60 ng/mL Tm. Cells were collected at the indicated times and subjected to western blotting analysis. A and B: Expression of GRP78, CHOP, BMAL1, ATF6, ATF4, and phospho-IRE1 in NIH3T3 cells treated or not with Tm at the indicated times. C: The ratio of each protein to β-actin was determined from the densities of the immunoreactive bands, and the results are shown as a bar graph. All data are presented as the means ± SE ($n = 3$). * $P < 0.05$, ** $P < 0.01$ vs. Cont at each time point.

stress by preventing N-linked glycosylation in the ER. We thus examined whether the Tg-/Tm-induced repressive effect on circadian clock gene transcription involves ER stress signaling, rather than being a direct effect. 4-Phenylbutyric acid (1 μM), a chemical chaperone that can decrease the ER stress response and acts as a histone deacetylase inhibitor [45], was used to attenuate Tg- or Tm-induced ER stress in NIH3T3 cells. As shown in the reduction of GRP78, ATF6, and ATF4 protein levels, the Tg- or Tm-induced ER stress activation was significantly alleviated by co-administration with 4-PBA (Fig. 6A). In addition, the qPCR results showed that the reduction in the mRNA expression levels of circadian clock genes (*Bmal1*, *Per2*, *Nr1d1*, and *Dbp*) in Tg/Tm treated NIH3T3 cells were partially rescued with the addition of 4-PBA (Fig. 6B). Notably, the addition of 4-PBA also partially restored the amplitude of *Bmal1-Luc* oscillations in Tg-/Tm-treated NIH3T3 cells (Fig. 6C), providing further evidence of the regulation of the circadian clockwork by ER stress.

3.6. The inhibitory effect of ER stress activation on the transcription of circadian clock genes does not involve ATF6

ATF6 protein levels underwent an obvious increase after Tg treatment in NIH3T3 cells. To understand the effects of ATF6 signaling on ER stress regulation of the cellular clockwork, the effects of ATF6 knockdown were evaluated in NIH3T3 cells using siRNA. Three sequences targeting ATF6 mRNA as well as a non-silencing RNA (NC) were constructed and successfully transfected into NIH3T3 cells for 60 h. qPCR revealed that ATF6 mRNA levels were reduced by approximately 90% with all three ATF6 siRNAs (Fig. 7A). Western blotting revealed a 50% reduction in ATF6 protein levels in NIH3T3 cells by all three ATF6 siRNAs (Fig. 7B). Therefore, a mixture of the three *Atf6* siRNAs was used to further evaluate the effects of ATF6 knockdown in Tg-treated NIH3T3 cells. As shown in Fig. 7C, there was a significant reduction in ATF6 and GRP78 protein levels in the Tg + Si group compared to the Tg group. However, ATF6 knockdown in Tg-treated NIH3T3 cells did not significantly alter the mRNA expression levels of circadian clock genes (*Bmal1*, *Dbp*, *Per2*, and *Nr1d1*) or amplitude of *Bmal1-Luc* oscillations compared to the Tg group (Fig. 7D, E). The results suggest that ATF6 signaling does not play an important role in ER stress regulation of the cellular circadian clockwork.

3.7. ATF4 knock-down partially rescues Bmal1-Luc oscillation amplitudes and the mRNA expression levels of circadian clock genes in Tg-treated NIH3T3 cells

ATF4 is an important component of ER stress signaling, and the ATF4 protein levels also showed a clear increase in NIH3T3 cells

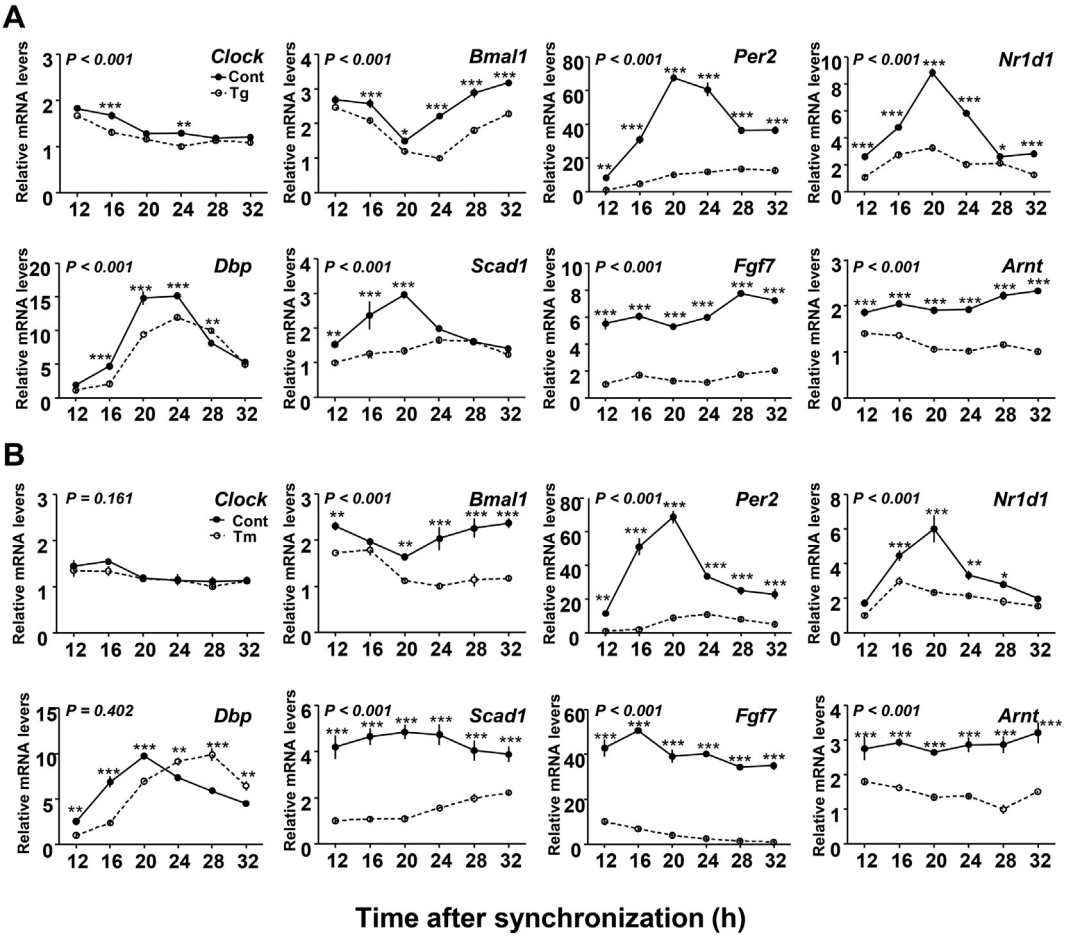

Fig. 5. mRNA expression profiles of circadian clock and clock-controlled genes in Tg- or Tm-treated NIH3T3 cells.
NIH3T3 cells were first synchronized using 100 nM DXM for 2 h, and were then treated with 60 nM Tg or 60 ng/mL Tm. Cell samples were collected at the indicated times for qPCR analysis. A and B: mRNA expression profiles of circadian clock and clock-controlled genes in Tg- or Tm-treated NIH3T3 cells. Each value represents the mean ± SE of three independent determinations. Two-way ANOVA followed a Holm-Sidak test were performed to investigate the main effects of different treatments on gene expression compared to the Cont group. Differences were considered significant at $P < 0.05$. * $P < 0.05$, ** $P < 0.01$, *** $P < 0.001$ vs. Cont at each time point.

following Tg treatment. To investigate the effects of ATF4 signaling on the regulation of the cellular circadian clockwork, the effects of ATF4 knockdown in NIH3T3 cells were also evaluated using siRNA. Three sequences targeting *Atf4* mRNA as well as a non-silencing RNA (NC) were constructed and successfully transfected into NIH3T3 cells for 60 h. qPCR revealed that *Atf4* mRNA levels were reduced by approximately 70% with all three *Atf4* siRNAs (Fig. 8A). Western blotting showed that ATF4 protein levels were reduced by > 75% in the S2 group (Fig. 8B); therefore, the S2 *Atf4* siRNA was used to further evaluate the effects of ATF4 in NIH3T3 cells. As shown in Fig. 8C, ATF4 knockdown significantly downregulated ATF4 and GRP78 protein expression in the Tg + Si group compared to the Tg group. Notably, ATF4 knockdown in Tg-treated NIH3T3 cells partially rescued the mRNA expression levels of circadian clock genes (*Bmal1*, *Per2*, *Dbp*, and *Nr1d1*) as well as *Bmal1-Luc* oscillation amplitudes (Fig. 8D, E) compared to the Tg group. The results revealed that ER stress regulation of the circadian clockwork is dependent on the ATF4 axis, at least in part.

4. Discussion

In the last two decades, substantial evidence has revealed that ER stress and circadian clockwork signaling both play important roles in cell proliferation, metabolism, and survival. However, the molecular connections between these two signaling pathways have remained largely unclear. In the present study, we investigated the mechanisms underlying ER stress signaling-mediated regulation of the circadian clockwork utilizing an ER stress perturbation NIH3T3 cell model, real-time monitoring of *Bmal1* promoter-driven bioluminescence, and RNAi. Our results show that Tg-/Tm-induced ER stress strikingly inhibited circadian clock and clock-controlled gene transcription and impaired their circadian rhythmicity. Moreover, 4-PBA significantly attenuated the repressive effect of Tg/Tm on the transcription of circadian clock genes in NIH3T3 cells, rescuing the mRNA expression levels of circadian clock gene and amplitude of *Bmal1-Luc* oscillations, at least in part. More importantly, knockdown of ATF4, but not ATF6, partially rescued the expression of circadian clock genes and amplitude of *Bmal1-Luc* oscillations in Tg-treated NIH3T3 cells. The present data demonstrate that ER stress signaling regulates cellular circadian clockwork via an ATF4-dependent mechanism.

To investigate the ER stress signaling-mediated regulation of the circadian clockwork, we used two classical ER stress inducers, Tg and Tm, to establish an ER stress model in NIH3T3 cells. Considering their potential cytotoxicity, we first determined reasonable Tg/Tm treatment concentrations that could trigger cellular ER stress without significantly affecting cell viability. The CCK-8 assay revealed that treatment with 60 nM Tg and 60 ng/mL Tm did not significantly decrease cell viability in NIH3T3 cells compared to the Cont group. Additional experiments using immunofluorescence and western blotting confirmed the successful induction of ER stress in NIH3T3 cells, showing the upregulation of ER stress signaling pathways. Our results agree with those of a

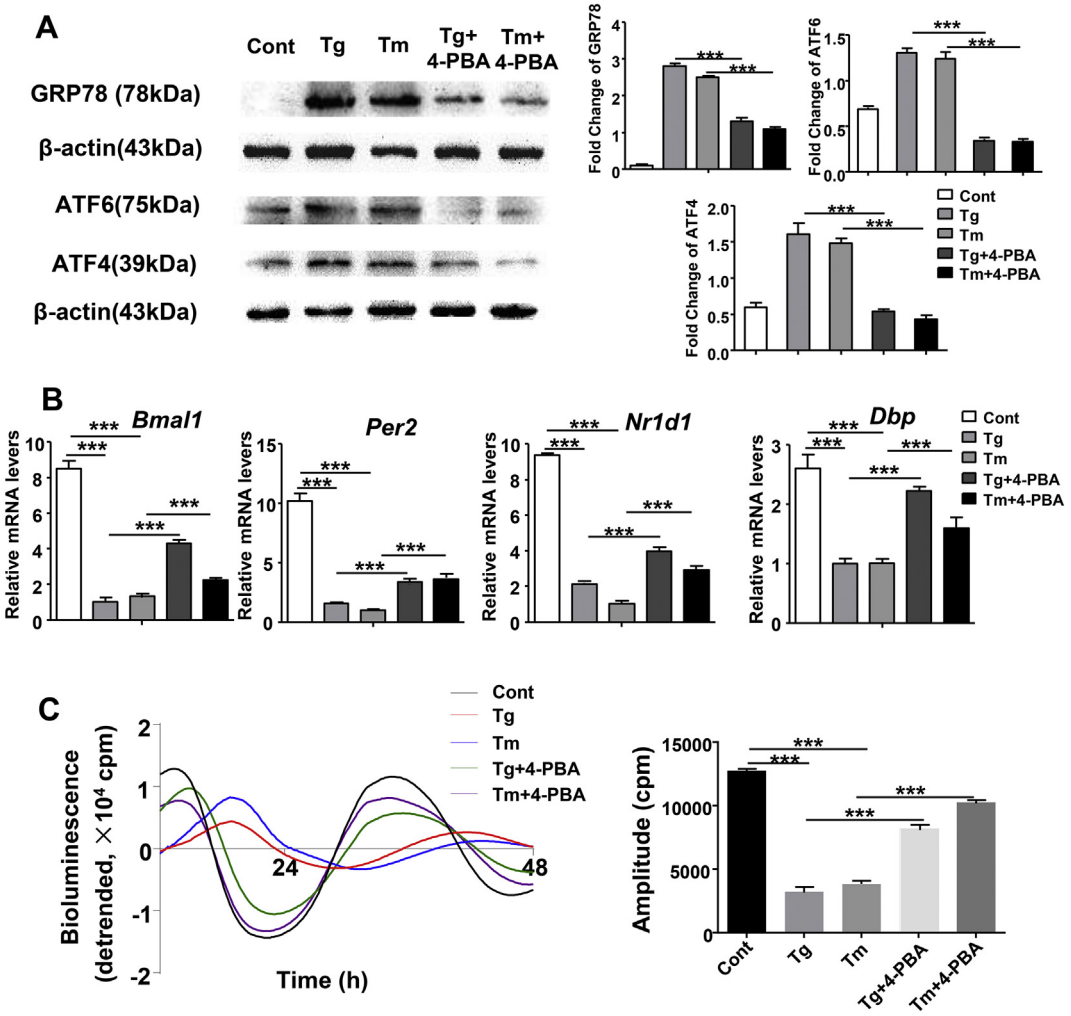

Fig. 6. Effect of 4-PBA on Tg- or Tm-induced downregulation of the circadian clockwork in NIH3T3 cells.
A and B: Western blotting and qPCR analysis of the effect of 4-PBA on ER stress and circadian clock signaling pathways in Tg/Tm treated NIH3T3 cells. Non-synchronized NIH3T3 cells were incubated with Tg (60 nM) or Tm (60 ng/mL) with or without co-administration of 4-PBA (1 μM). Cell samples were collected at 24 h after treatment. The expression of GRP78, ATF6, and ATF4 was examined by western blot. Representative blots and quantitative analysis from three independent experiments are shown. All data are presented as the means ± SE ($n = 3$). *** $P < 0.001$ vs. Tg or Tm. mRNA expression levels of circadian clock genes were examined by qPCR. Each value represents the mean ± SE of 3 independent determinations. *** $P < 0.001$. C: Effect of 4-PBA on *Bmal1-Luc* oscillation amplitudes in Tg or Tm-treated NIH3T3 cells. The NIH3T3 cells were synchronized with 100 nM DXM for 2 h and then incubated with Tg (60 nM) or Tm (60 ng/mL) with or without the presence of 4-PBA (1 μM). Luciferase activity was monitored chronologically with a Kronos Dio AB-2550 luminometer. Amplitudes are generated by the cosinor method based on data for the first 48 h. Results are the means ± SE ($n = 6$). *** $P < 0.001$.

previous report showing that 100 nM Tg or 100 ng/mL Tm treatment could trigger ER stress by upregulating GRP78 in NIH3T3 cells [44].

Thapsigargin activates cellular ER stress by inhibiting the transport of Ca^{2+} to the ER [13]. Calcium signaling is strongly involved in regulating the expression of the circadian clock gene *Per1* [46,47]. The effect of Tg treatment on the circadian clockwork in NIH3T3 cells does not exclude the possibility that Tg regulates the circadian clockwork by inhibiting the transport of Ca^{2+} to the ER lumen. Therefore, we also used Tm, an inhibitor of N-linked glycosylation in the ER [15], to investigate the ER stress signaling-mediated regulation of the circadian clockwork. Interestingly, Tg or Tm treatment impaired *Bmal1-Luc* circadian oscillations in NIH3T3 cells, highlighting the potential connection between ER stress signaling and the circadian clockwork. Additionally, both Tg and Tm strikingly inhibited the transcription of some canonical circadian clock and clock-controlled genes and also significantly decreased BMAL1 protein levels in NIH3T3 cells, providing plausible evidence that Tg-/Tm-mediated ER stress activation downregulates the cellular clockwork. To verify that Tg-/Tm-mediated inhibition of the cellular clockwork in NIH3T3 cells is involved ER stress activation, we further measured the effect of 4-PBA (an ER stress inhibitor) on the cellular circadian clockwork in Tg- or Tm-treated NIH3T3 cells. As expected, 4-PBA efficiently attenuated GRP78, ATF4, and ATF6 expression as a reflection of reduced ER stress in Tg- or Tm-treated NIH3T3 cells. Notably, 4-PBA alleviated the Tg-/Tm-induced downregulation of circadian clock gene transcription and *Bmal1-Luc* oscillation amplitudes in NIH3T3 cells. Collectively, the results indicate that ER stress activation inhibits the transcription of cellular circadian clock and clock-controlled genes.

The ATF6 protein is an ER stress-regulated transmembrane transcription factor that activates the transcription of ER molecules. Accumulation of misfolded proteins in the ER results in the proteolytic cleavage of ATF6, the cytosolic portion of which translocates to the nucleus and elicits the transcription of ER chaperones [48]. Accordingly, our results showed that ATF6 expression apparently increased when UPR signaling was induced by Tg/Tm in NIH3T3 cells. To investigate whether ATF6 acts as an integrator between ER stress and circadian clockwork pathways, we knocked down ATF6 protein expression by siRNA transfection in Tg-treated NIH3T3 cells. However,

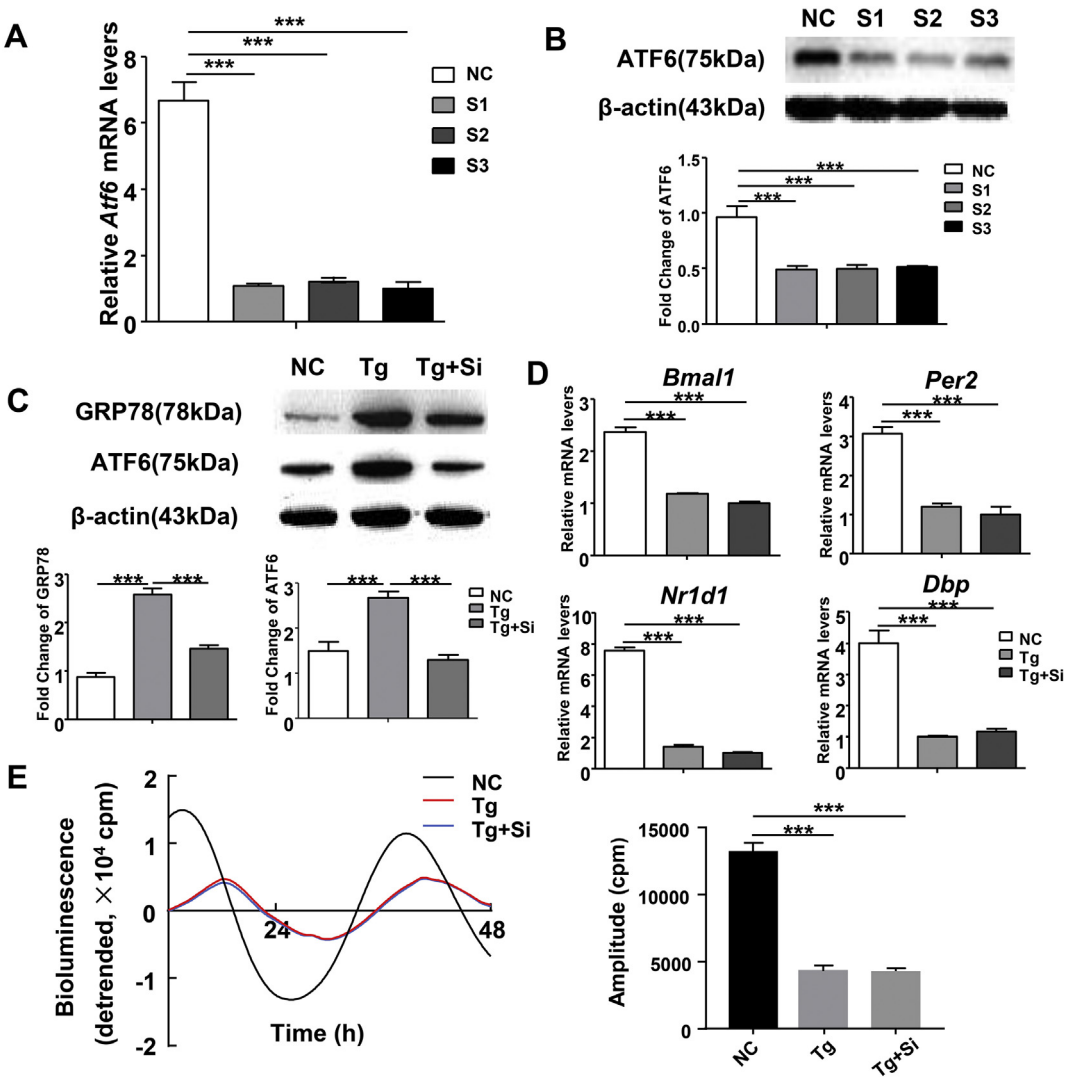

Fig. 7. Effects of ATF6 knockdown on the circadian clockwork in Tg-treated NIH3T3 cells.
A and B: qPCR and western blotting analysis of the efficiency of ATF6 siRNA knockdown in NIH3T3 cells. The cells were transfected with S1–3 siRNAs against ATF6 or non-silencing RNA (NC) for 12 h in transfection medium and the culture medium was then changed to normal medium containing 10% FBS and 1 × AA for 48 h. Each value represents the mean ± SE of 3 independent determinations. *** $P < 0.001$ vs. NC. C and D: Effects of *Atf6* siRNA transfection on ER stress and circadian clock signaling pathways in Tg-treated NIH3T3 cells. The cells were transfected with a mixture of *Atf6* siRNAs or non-silencing RNA (NC) for 12 h. The non-synchronized cells of the *Atf6* siRNA and NC groups were then treated with Tg (60 nM) for 48 h. The GRP78 and ATF6 protein levels were examined by western blot. Representative blots and quantitative analysis from three independent experiments are shown. All data are presented as the means ± SE ($n = 3$). * $P < 0.05$, *** $P < 0.001$. The mRNA expression levels of circadian clock genes were examined by qPCR. Each value represents the mean ± SE of three independent determinations. *** $P < 0.001$. E: Effect of *Atf6* siRNA transfection on *Bmal1-Luc* oscillation amplitudes in Tg-treated NIH3T3 cells. The cells were transfected with *Atf6* siRNAs or non-silencing RNAs, and then treated with 100 nM DXM for 2 h. The *Atf6* siRNA-treated cells were then treated with 60 nM Tg (Tg + Si). The non-silencing RNA-treated cells were then treated or not (NC) with 60 nM Tg. Luciferase activity was monitored chronologically with a Kronos Dio AB-2550 luminometer. Amplitudes are generated by the cosinor method based on the data for the first 48 h. Results are the means ± SE ($n = 6$). *** $P < 0.001$.

transfection with siRNA targeting ATF6 in Tg-treated NIH3T3 cells did not significantly change the mRNA expression levels of the circadian clock genes or the amplitude of *Bmal1-Luc* oscillations compared to Tg treatment alone. These data suggest that the ATF6 axis of the ER stress signaling pathway might not be involved in the ER stress regulation of the cellular circadian clockwork.

In addition to ATF6, ATF4 also acts as an important transcriptional activator of UPR target genes [49]. We observed an apparent increase in the levels of the ATF4 protein when ER stress was induced by Tg/Tm treatment in NIH3T3 cells. We further examined whether ATF4 signaling is involved in ER stress regulation of the cellular circadian clockwork using *Atf4* siRNA transfection. Surprisingly, ATF4 knockdown in Tg-treated NIH3T3 cells partially rescued the mRNA expression levels of circadian clock genes and *Bmal1-Luc* oscillation amplitudes compared to the Tg group. A very recent report revealed that UPR signaling directly regulates the core circadian clock through the PERK-eIF2α-ATF4-miR-211 axis [38]. Mechanistically, the ATF4-inducible micro-RNA, miR-211, directly suppresses both BMAL1 and CLOCK. In line with this elegant study, our current results provide additional evidence that ER stress-mediated induction of the UPR inhibits the cellular circadian clockwork via an ATF4-dependent mechanism, at least in part. However, whether other branches downstream of UPR signaling regulate the cellular circadian clockwork remains unclear.

Aryl hydrocarbon receptor nuclear translocator (ARNT) is a member of the bHLH-PAS family, and *Arnt* mRNA expression has been shown to fluctuate significantly in a circadian manner in mouse pancreatic islets [50]. The FGF7 protein, a member of the fibroblast growth factor

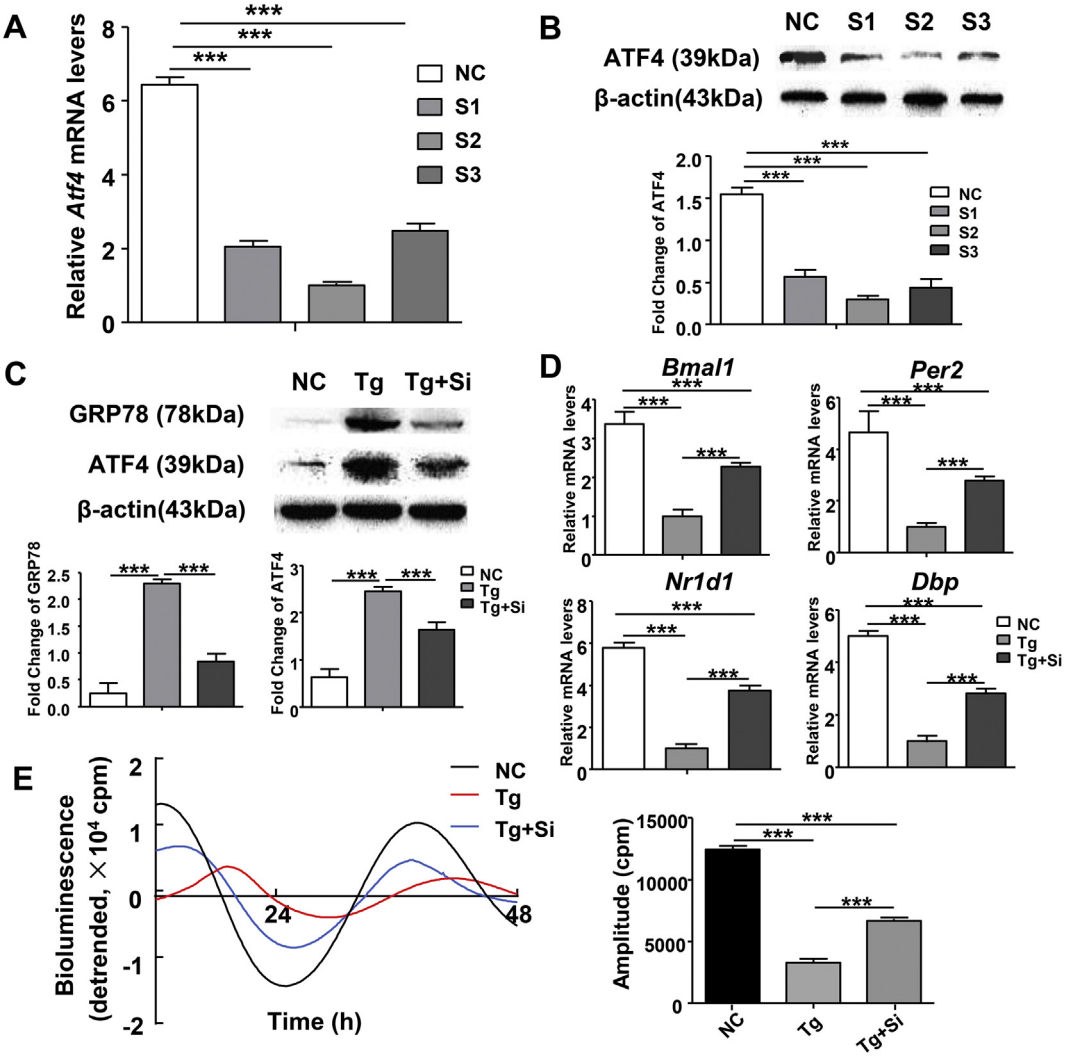

Fig. 8. Effects of ATF4 knockdown on the circadian clockwork in Tg-treated NIH3T3 cells.
A and B: qPCR and western blotting analysis of the efficiency of ATF4 siRNA knockdown in NIH3T3 cells. The cells were transfected with S1–3 siRNAs against ATF4 or a non-silencing RNA (NC) for 12 h in transfection medium, and the culture medium was then changed to normal medium containing 10% FBS and 1 × AA for 48 h. Each value represents the mean ± SE of three independent determinations. *** $P < 0.001$ vs. NC. C and D: Effects of *Atf4* siRNA transfection on ER stress and circadian clock signaling pathways in Tg-treated NIH3T3 cells. The cells were transfected with the S2 *Atf4* siRNA or non-silencing RNA (NC) for 12 h. The non-synchronized cells of the *Atf4* siRNA groups and the NC group were then treated with Tg (60 nM) for 48 h. The GRP78 and ATF4 protein levels were examined by western blot. Representative blots and quantitative analysis from three independent experiments are shown. All data are presented as the means ± SE ($n = 3$). * $P < 0.05$, *** $P < 0.001$. The mRNA expression levels of circadian clock genes were examined by qPCR. Each value represents the mean ± SE of three independent determinations. *** $P < 0.001$. E: Effect of *Atf4* siRNA transfection on *Bmal1-Luc* oscillation amplitudes in Tg-treated NIH3T3 cells. The cells were transfected with the S2 *Atf4* siRNA or non-silencing RNA and treated with 100 nM DXM for 2 h. The *Atf4* siRNA-treated cells were then treated with 60 nM Tg (Tg + Si). The non-silencing RNA-treated cells were then treated or not (NC) with 60 nM Tg. Luciferase activity was monitored chronologically with a Kronos Dio AB-2550 luminometer. Amplitudes are generated by the cosinor method based on the data for the first 48 h. Results are the means ± SE ($n = 6$). *** $P < 0.001$.

family, possesses broad mitogenic and cell survival activities [51]. SCAD1, also termed stearoyl-CoA desaturase 1, is a fatty acid metabolism enzyme, and knockout of *Per1* increases *Scad1* mRNA levels in mice [52]. *Arnt*, *Fgf7,* and *Scad1* are all clock-controlled genes [53] and, in the present study, both Tg and Tm strikingly decreased the mRNA levels of these three genes as well as the levels of circadian clock genes (*Bmal1*, *Per2*, *Nr1d1*, and *Dbp*). Consequently, it is reasonable to speculate that ER stress signaling regulates circadian physiology through the direct action of circadian clock genes and the indirect action of their downstream clock-controlled genes. Endoplasmic reticulum stress-mediated impairment of the circadian clockwork may directly damage fatty acid metabolism, cell survival activities, embryonic development, and other processes and further studies should explore these possibilities.

Our previous studies showed that there is a functional circadian clockwork in mouse Leydig cells, mature rat granulose cells, and uterus endometrial stromal cells of pregnant rats [54–56]. Furthermore, our prior studies also showed that ER stress signaling regulates the cell cycle and hormone secretion in mouse granulose cells [57]. Since the current study revealed cross-talk between ER stress signaling and the circadian clockwork, this suggests that ER stress may interact with the circadian clockwork to regulate reproductive physiological functions. Considering the complexity of the circadian clockwork and the reproductive system, the interactions among specific molecular mechanisms in different reproductive cells should be examined. Moreover, the specific contribution of the UPR/circadian clock network should be fully examined in other cell types.

5. Conclusions

In conclusion, ER stress activation represses circadian clock and clock-controlled gene transcription via an ATF4-dependent mechanism. Considering that ER stress-mediated induction of UPR signaling occurs frequently in various cells and tissues in response to different stimuli, the present findings expand our understanding of the mechanisms underlying how ER stress affects cellular physiological functions through regulation of the circadian clockwork.

Conflicts of interest

None.

Acknowledgements

We are grateful to Dr. Steven Brown (University of Zurich, Zurich, Switzerland) for providing the pLV6-*Bmal1-Luc* plasmid.

Funding

This work was supported by grants from the National Natural Science Foundation of China (Grant No. 31602125, 31771301, to H. Chen; Grant No. 31772817, to Y. Jin); China Postdoctoral Science Foundation (Grant No. 2018T111112, 2017M61065, to H. Chen); Shaanxi Postdoctoral Science Foundation (Grant No. 2017BSHEDZZ105, to H. Chen); The Fundamental Research Funds for the Central Universities (Grant No. 2452017292, to H. Chen); The Scientific Research Foundation for Talents of Shaanxi (Grant No. A279021712, to H. Chen); and The Scientific Research Foundation for Talents of Northwest A&F University (Grant No. Z11021601, to H. Chen). The sponsors had no role in the analysis or decision to publish the work.

Author contributions

H.C. and Y.J. conceived and supervised the study; L.G., H.C., and Y.J. designed the experiments; L.G. and H.C. performed the experiments and analyzed data; C.L., Y.X., D.Y., M.Z., D.Z., W.L., and A.W. helped with experiments; L.G. and H.C. wrote the manuscript; H.C. and L.G. made manuscript revisions; H.C. and Y.J. approved the final version of the manuscript.

Appendix A. Supplementary data

Supplementary data to this article can be found online at https://doi.org/10.1016/j.cellsig.2019.01.008.

References

[1] C. Hammond, I. Braakman, A. Helenius, Role of N-linked oligosaccharide recognition, glucose trimming, and calnexin in glycoprotein folding and quality control, Proc. Natl. Acad. Sci. U. S. A. 91 (3) (1994) 913–917.
[2] O. Pluquet, A. Pourtier, C. Abbadie, The unfolded protein response and cellular senescence. A review in the theme: cellular mechanisms of endoplasmic reticulum stress signaling in health and disease, Am. J. Phys. Cell Physiol. 308 (6) (2015) C415–C425.
[3] A.M. Gorman, S.J.M. Healy, R. Jager, A. Samali, Stress management at the ER: regulators of ER stress-induced apoptosis, Pharmacol. Ther. 134 (3) (2012) 306–316.
[4] C. Hetz, E. Chevet, S.A. Oakes, Proteostasis control by the unfolded protein response, Nat. Cell Biol. 17 (7) (2015) 829–838.
[5] K.A. Moore, J. Hollien, The unfolded protein response in secretory cell function, Annu. Rev. Genet. 46 (2012) 165–183.
[6] J.W. Brewer, Regulatory crosstalk within the mammalian unfolded protein response, Cell. Mol. Life Sci. 71 (6) (2014) 1067–1079.
[7] H.P. Harding, Y. Zhang, D. Ron, Protein translation and folding are coupled by an endoplasmic-reticulum-resident kinase, Nature 397 (6716) (1999) 271–274.
[8] Y. Ma, J.W. Brewer, J.A. Diehl, L.M. Hendershot, Two distinct stress signaling pathways converge upon the CHOP promoter during the mammalian unfolded protein response, J. Mol. Biol. 318 (5) (2002) 1351–1365.
[9] C. Hetz, The unfolded protein response: controlling cell fate decisions under ER stress and beyond, Nat. Rev. Mol. Cell Biol. 13 (2) (2012) 89–102.
[10] M. Flamment, E. Hajduch, P. Ferré, F. Foufelle, New Insights in to ER Stress Induced Insulin Resistance, (2012).
[11] W. Tirasophon, A.A. Welihinda, R.J. Kaufman, A stress response pathway from the endoplasmic reticulum to the nucleus requires a novel bifunctional protein kinase/endoribonuclease (Ire1p) in mammalian cells, Genes Dev. 12 (12) (1998) 1812–1824.
[12] K. Haze, H. Yoshida, H. Yanagi, T. Yura, K. Mori, Mammalian transcription factor ATF6 is synthesized as a transmembrane protein and activated by proteolysis in response to endoplasmic reticulum stress, Mol. Biol. Cell 10 (11) (1999) 3787–3799.
[13] M. Treiman, C. Caspersen, S.B. Christensen, A tool coming of age: thapsigargin as an inhibitor of sarcoendoplasmic reticulum Ca^{2+}-ATPases, Trends Pharmacol. Sci. 19 (4) (1998) 131–135.
[14] E. Kmonickova, P. Melkusova, J. Harmatha, K. Vokac, H. Farghali, Z. Zidek, Inhibitor of sarco-endoplasmic reticulum Ca^{2+}-ATPase thapsigargin stimulates production of nitric oxide and secretion of interferon-gamma, Eur. J. Pharmacol. 588 (1) (2008) 85–92.
[15] M.A. Lehrman, Oligosaccharide-based information in endoplasmic reticulum quality control and other biological systems, J. Biol. Chem. 276 (12) (2001) 8623–8626.
[16] H.J. Hwang, T.W. Jung, J.Y. Ryu, H.C. Hong, H.Y. Choi, J.A. Seo, S.G. Kim, N.H. Kim, K.M. Choi, D.S. Choi, S.H. Baik, H.J. Yoo, Dipeptidyl petidase-IV inhibitor (gemigliptin) inhibits tunicamycin-induced endoplasmic reticulum stress, apoptosis and inflammation in H9c2 cardiomyocytes, Mol. Cell. Endocrinol. 392 (1–2) (2014) 1–7.
[17] U. Ozcan, E. Yilmaz, L. Ozcan, M. Furuhashi, E. Vaillancourt, R.O. Smith, C.Z. Gorgun, G.S. Hotamisligil, Chemical chaperones reduce ER stress and restore glucose homeostasis in a mouse model of type 2 diabetes, Science 313 (5790) (2006) 1137–1140.
[18] G.S. Zode, M.H. Kuehn, D.Y. Nishimura, C.C. Searby, K. Mohan, S.D. Grozdanic, K. Bugge, M.G. Anderson, A.F. Clark, E.M. Stone, V.C. Sheffield, Reduction of ER stress via a chemical chaperone prevents disease phenotypes in a mouse model of primary open angle glaucoma, J. Clin. Invest. 125 (8) (2015) 3303.
[19] X.G. Wang, P.F. Lin, Y. Li, C.X. Xiang, Y.L. Yin, Z. Chen, Y. Du, D. Zhou, Y.P. Jin, A.H. Wang, Brucella suis vaccine strain 2 induces endoplasmic reticulum stress that affects intracellular replication in goat trophoblast cells in vitro, Front. Cell Infect. Microbiol. 6 (2016) 19.
[20] C. Dibner, U. Schibler, U. Albrecht, The mammalian circadian timing system: organization and coordination of central and peripheral clocks, Annu. Rev. Physiol. 72 (2010) 517–549.
[21] A. Sancar, R. Ye, C.P. Selby, N. Ozturk, Y. Annayev, Biochemical analysis of the canonical model for the mammalian circadian clock, J. Biol. Chem. 286 (29) (2011) 25891–25902.
[22] T. Ueyama, K.E. Krout, X. Van Nguyen, V. Karpitskiy, A. Kollert, T.C. Mettenleiter, A.D. Loewy, Suprachiasmatic nucleus: a central autonomic clock, Nat. Neurosci. 2 (12) (1999) 1051–1053.
[23] M.A. Henson, T.L. To, E.D. Herzog, F.J. Doyle, A molecular model for intercellular synchronization in the mammalian circadian clock, Biophys. J. 92 (11) (2007) 3792–3803.
[24] U. Albrecht, Timing to perfection: the biology of central and peripheral circadian clocks, Neuron 74 (2) (2012) 246–260.
[25] N.A. Huang, Y. Chelliah, Y.L. Shan, C.A. Taylor, S.H. Yoo, C. Partch, C.B. Green, H. Zhang, J.S. Takahashi, Crystal structure of the heterodimeric CLOCK:BMAL1 transcriptional activator complex, Science 337 (6091) (2012) 189–194.
[26] P. Lebeau, A. Al-Hashimi, S. Sood, S. Lhotak, P. Yu, G. Gyulay, G. Pare, S.R.W. Chen, B. Trigatti, A. Prat, N.G. Seidah, R.C. Austin, Endoplasmic reticulum stress and Ca2+ depletion differentially modulate the sterol regulatory protein PCSK9 to control lipid metabolism, J. Biol. Chem. 292 (4) (2017) 1510–1523.
[27] Y.M. Li, Y.S. Guo, J. Tang, J.L. Jiang, Z.N. Chen, New insights into the roles of CHOP-induced apoptosis in ER stress, Acta Biochim. Biophys. Sin. 46 (8) (2014) 629–640.
[28] E. Kania, B. Pajak, A. Orzechowski, Calcium homeostasis and ER stress in control of autophagy in cancer cells, Biomed. Res. Int. 1155 (2015) 352794.
[29] Y.Z. Yang, J. Chen, H. Wu, X.Y. Pei, Q. Chang, W.Z. Ma, H.M. Ma, C.C. Hei, X.M. Zheng, Y.F. Cai, C.J. Zhao, J. Yu, Y.R. Wang, The increased expression of connexin and VEGF in mouse ovarian tissue vitrification by follicle stimulating hormone, Biomed. Res. Int. 1155 (2015) (2015) 397264.
[30] H.J. Park, S.J. Park, D.B. Koo, S.R. Lee, I.K. Kong, J.W. Ryoo, Y.I. Park, K.T. Chang, D.S. Lee, Progesterone production is affected by unfolded protein response (UPR) signaling during the luteal phase in mice, Life Sci. 113 (1–2) (2014) 60–67.
[31] S. Gaddameedhi, J.T. Reardon, R. Ye, N. Ozturk, A. Sancar, Effect of circadian clock mutations on DNA damage response in mammalian cells, Cell Cycle 11 (18) (2012) 3481–3491.
[32] F. Kalfalah, L. Janke, A. Schiavi, J. Tigges, A. Ix, N. Ventura, F. Boege, H. Reinke, Crosstalk of clock gene expression and autophagy in aging, Aging-Us 8 (9) (2016) 1876–1895.
[33] S. Sahar, P. Sassone-Corsi, Regulation of metabolism: the circadian clock dictates the time, Trends Endocrinol. Metab. 23 (1) (2012) 1–8.
[34] H. Chen, L. Zhao, M. Kumazawa, N. Yamauchi, Y. Shigeyoshi, S. Hashimoto, M.-A. Hattori, Downregulation of core clock gene *Bmal1* attenuates expression of progesterone and prostaglandin biosynthesis-related genes in rat luteinizing granulosa cells, Am. J. Physiol. Cell Physiol. 304 (12) (2013) C1131–C1140.
[35] B. Grimaldi, M.M. Bellet, S. Katada, G. Astarita, J. Hirayama, R.H. Amin,

J.G. Granneman, D. Piomelli, T. Leff, P. Sassone-Corsi, PER2 controls lipid metabolism by direct regulation of PPARgamma, Cell Metab. 12 (5) (2010) 509–520.
[36] F. Gachon, G. Cretenet, M. Le Clech, Circadian clock-coordinated 12 hr period rhythmic activation of the IRE1 alpha pathway controls lipid metabolism in mouse liver, Cell Metab. 11 (1) (2010) 47–57.
[37] G.S. Yuan, B.X. Hua, T.T. Cai, L.R. Xu, E.M. Li, Y.Q. Huang, N. Sun, Z.Q. Yan, C. Lu, R.Z. Qian, Clock mediates liver senescence by controlling ER stress, Aging-Us 9 (12) (2017) 2647–2665.
[38] Y.W. Bu, A. Yoshida, N. Chitnis, B.J. Altman, F. Tameire, A. Oran, V. Gennaro, K.E. Armeson, S.B. McMahon, G.B. Wertheim, C.V. Dang, D. Ruggero, C. Koumenis, S.Y. Fuchs, J.A. Diehl, A PERK-miR-211 axis suppresses circadian regulators and protein synthesis to promote cancer cell survival, Nat. Cell Biol. 20 (1) (2018) 104–105.
[39] D. Zhou, F.J. Zhi, M.Z. Qi, F.R. Bai, G. Zhang, J.M. Li, H. Liu, H.T. Chen, P.F. Lin, K.Q. Tang, W. Liu, Y.P. Jin, A.H. Wang, Brucella induces unfolded protein response and inflammatory response via GntR in alveolar macrophages, Oncotarget 9 (4) (2018) 5184–5196.
[40] S.A. Brown, F. Fleury-Olela, E. Nagoshi, C. Hauser, C. Juge, C.A. Meier, R. Chicheportiche, J.M. Dayer, U. Albrecht, U. Schibler, The period length of fibroblast circadian gene expression varies widely among human individuals, PLoS Biol. 3 (10) (2005) 1813–1818.
[41] M. Hirata, P.J. He, N. Shibuya, M. Uchikawa, N. Yamauchi, S. Hashimoto, M.A. Hattori, Progesterone, but not estradiol, synchronizes circadian oscillator in the uterus endometrial stromal cells, Mol. Cell. Biochem. 324 (1–2) (2009) 31–38.
[42] H. Chen, L. Zhao, G. Chu, G. Kito, N. Yamauchi, Y. Shigeyoshi, S. Hashimoto, M.-A. Hattori, FSH induces the development of circadian clockwork in rat granulosa cells via a gap junction protein Cx43-dependent pathway, Am. J. Physiol. Endocrinol. Metab. 304 (6) (2013) E566–E575.
[43] D. Yang, T. Jiang, J. Liu, B. Zhang, P. Lin, H. Chen, D. Zhou, K. Tang, A. Wang, Y. Jin, CREB3 regulatory factor -mTOR-autophagy regulates goat endometrial function during early pregnancy, Biol. Reprod. 98 (5) (2018) 713–721.
[44] V.M. Labunskyy, M.H. Yoo, D.L. Hatfield, V.N. Gladyshev, Sep15, a thioredoxin-like selenoprotein, is involved in the unfolded protein response and differentially regulated by adaptive and acute ER stresses, Biochemistry 48 (35) (2009) 8458–8465.
[45] A. Malo, B. Kruger, B. Goke, C.H. Kubisch, 4-Phenylbutyric acid reduces endoplasmic reticulum stress, trypsin activation, and acinar cell apoptosis while increasing secretion in rat pancreatic acini, Pancreas 42 (1) (2013) 92–101.
[46] M. Akiyama, Y. Minami, T. Nakajima, T. Moriya, S. Shibata, Calcium and pituitary adenylate cyclase-activating polypeptide induced expression of circadian clock gene mPer1 in the mouse cerebellar granule cell culture, J. Neurochem. 78 (3) (2001) 499–508.
[47] A. Balsalobre, L. Marcacci, U. Schibler, Multiple signaling pathways elicit circadian gene expression in cultured Rat-1 fibroblasts, Curr. Biol. 10 (20) (2000) 1291–1294.
[48] M.Q. Li, P. Baumeister, B. Roy, T. Phan, D. Foti, S.Z. Luo, A.S. Lee, ATF6 as a transcription activator of the endoplasmic reticulum stress element: thapsigargin stress-induced changes and synergistic interactions with NF-Y and YY1, Mol. Cell. Biol. 20 (14) (2000) 5096–5106.
[49] S. Dey, T.D. Baird, D. Zhou, L.R. Palam, D.F. Spandau, R.C. Wek, Both transcriptional regulation and translational control of ATF4 are central to the integrated stress response, J. Biol. Chem. 285 (43) (2010) 33165–33174.
[50] H. Nakabayashi, Y. Ohta, M. Yamamoto, Y. Susuki, A. Taguchi, K. Tanabe, M. Kondo, M. Hatanaka, Y. Nagao, Y. Tanizawa, Clock-controlled output gene *Dbp* is a regulator of *Arnt/Hif-1* beta gene expression in pancreatic islet beta-cells, Biochem. Biophys. Res. Commun. 434 (2) (2013) 370–375.
[51] F. Belleudi, V. Purpura, S. Caputo, M.R. Torrisi, FGF7/KGF regulates autophagy in keratinocytes a novel dual role in the induction of both assembly and turnover of autophagosomes, Autophagy 10 (5) (2014) 803–821.
[52] T. Wang, P. Yang, Y.B. Zhan, L. Xia, Z.C. Hua, J.F. Zhang, Deletion of circadian gene *Per1* alleviates acute ethanol-induced hepatotoxicity in mice, Toxicology 314 (2–3) (2013) 193–201.
[53] G.J. Menger, G.C. Allen, N. Neuendorff, S.S. Nahm, T.L. Thomas, V.M. Cassone, D.J. Earnest, Circadian profiling of the transcriptome in NIH/3T3 fibroblasts: comparison with rhythmic gene expression in SCN2.2 cells and the rat SCN, Physiol. Genomics 29 (3) (2007) 280–289.
[54] H. Chen, G. Chu, L. Zhao, N. Yamauchi, Y. Shigeyoshi, S. Hashimoto, M.-A. Hattori, Rev-erbα regulates circadian rhythms and *Star* expression in rat granulosa cells as identified by the agonist GSK4112, Biochem. Biophys. Res. Commun. 420 (2) (2012) 374–379.
[55] H. Chen, L. Gao, Y. Xiong, D. Yang, C. Li, A. Wang, Y. Jin, Circadian clock and steroidogenic-related gene expression profiles in mouse Leydig cells following dexamethasone stimulation, Biochem. Biophys. Res. Commun. 483 (1) (2017) 294–300.
[56] H. Tasaki, L. Zhao, K. Isayama, H. Chen, N. Yamauchi, Y. Shigeyoshi, S. Hashimoto, M.-A. Hattori, Profiling of circadian genes expressed in the uterus endometrial stromal cells of pregnant rats as revealed by DNA microarray coupled with RNA interference, Front. Endocrinol. 4 (2013) 82.
[57] Y. Xiong, H. Chen, P. Lin, A. Wang, L. Wang, Y. Jin, ATF6 knockdown decreases apoptosis, arrests the S phase of the cell cycle, and increases steroid hormone production in mouse granulosa cells, Am. J. Phys. Cell Physiol. 312 (3) (2017) C341–C353.